AD-779 469

STRESS INTENSITY FACTORS FOR ELLIPTICAL CRACKS

Albert S. Kobayashi, et al

Washington University

AD-779469

DOCUMENT CONTROL DATA - R & D

(Security classification of title, body of abstract and indexing annotation must be entered when the overall report is classified)

1. ORIGINATING ACTIVITY (Corporate author)	2a. REPORT SECURITY CLASSIFICATION
University of Washington	Unclassified
	2b. GROUP Not applicable

3. REPORT TITLE

"Stress Intensity Factors for Elliptical Cracks"

4. DESCRIPTIVE NOTES (Type of report and inclusive dates)

Interim Technical Report No. 2, March 1974

5. AUTHOR(S) (First name, middle initial, last name)

Albert S. Kobayashi, Alfred N. Enetanya, and Rameshchandra C. Shah

6. REPORT DATE	7a. TOTAL NO. OF PAGES	7b. NO. OF REFS
September 1973	22	27

8a. CONTRACT OR GRANT NO.	9a. ORIGINATOR'S REPORT NUMBER(S)
Grant No. DA-ARO-D-31-124-73-G38	
b. PROJECT NO.	No. 2
None	
c.	9b. OTHER REPORT NO(S) (Any other numbers that may be assigned this report)
d.	Not applicable

10. DISTRIBUTION STATEMENT

Approved for public distribution

11. SUPPLEMENTARY NOTES	12. SPONSORING MILITARY ACTIVITY
Not applicable	Army Research Office - Durham

13. ABSTRACT

The combined use of a solution for an elliptical crack subjected to a polynomial distribution of internal pressure together with a free surface solution for the alternating method is reviewed in order to improve the efficiency of this numerical technique. Numerical differentiation to avoid deriving and computer programming of complex mathematical expressions is discussed. A criterion for maximum grid size for the free surface solution is proposed. Also optimum fittings of the first, second and third order polynomial distributions of internal pressure are considered.

Reproduced by
NATIONAL TECHNICAL
INFORMATION SERVICE
U S Department of Commerce
Springfield VA 22151

DDC
RECEIVED
MAY 21 1974
D

KEY WORDS	LINK A		LINK B		LINK C	
	ROLE	WT	ROLE	WT	ROLE	WT
Fracture Mechanics						
Stress Intensity Factor						
Three-Dimensional Elasticity						

DD FORM 1473 (BACK)
1 NOV 65

(PAGE 2)

FOREWORD

This Interim Technical Report No. 2 was prepared for presentation
at the Conference on the Prospects of Advanced Fracture Mechanics which
is to be held in Delft, Netherland, June 24 - 28, 1974, under the joint
sponsorship of the Metal Research Institute T. N. O. and Delft Univer-
sity of Technology in close cooperation with Lehigh University.

The figures in this report were reduced in compliance with the
format specified by the Seminar organizers.

Full-size, 8 1/2" x 11", figures can be obtained for numerical
computation by writing to the undersigned:

Professor Albert S. Kobayashi
Department of Mechanical Engineering
University cf Washington
Seattle, Washington 98195

THE FINDINGS OF THIS REPORT ARE NOT TO BE

CONSTRUED AS AN OFFICIAL DEPARTMENT OF THE

ARMY POSITION, UNLESS SO DESIGNATED BY OTHER

AUTHORIZED DOCUMENTS.

STRESS INTENSITY FACTORS FOR ELLIPTICAL CRACKS

A.S. Kobayashi, A.N. Enetanya, and R.C. Shah

University of Washington, Seattle, Washington 98195 and
The Boeing Aerospace Company, Seattle, Washington 98124

ABSTRACT

The combined use of a solution for an elliptical crack sub-
jected to internal pressure, which is represented by a polynomial
expression, together with a free surface solution for the alter-
nating method is reviewed and methods for improving the efficiency
of this numerical technique are proposed. Numerical differentia-
tion for avoiding the derivation and computer programming of com-
plex mathematical expressions is discussed. A criterion for max-
imum grid size for the free surface solution is proposed. Also
optimum fittings of the first, second and third order polynomial
distributions of internal pressure are considered.

INTRODUCTION

Post mortem failure analysis of fractured structural compo-
nents requires modeling of an embedded or surface flaw from which
fracture initiated. More often, these flaws can be approximated
by an ellipse and are located in regions of stress concentrations
or thin cross-section, such as those shown in Fig. 1, where the
stress gradient as well as the complex geometry of the structure
cannot be ignored. The elliptical crack and its interaction with
its adjacent or intersecting boundaries have thus been studied by
various investigators during the past ten years.

The earliest paper on stress intensity factor of an ellipti-
cal crack is that by Irwin[1] who then derived the approximate ex-
pression for the stress intensity factor at the point of deepest

(a) EMBEDDED ELLIPTICAL WELD DEFECT IN A FLANGE - WEB CONNECTION

(b) QUARTER-ELLIPTICAL FLAW AT A HOLE

(c) DEEP PART-ELLIPTICAL SURFACE FLAW

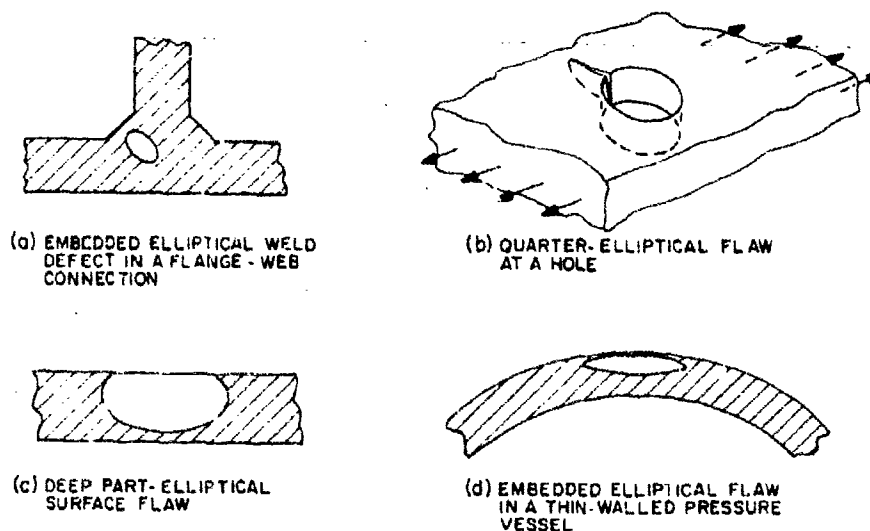(d) EMBEDDED ELLIPTICAL FLAW IN A THIN-WALLED PRESSURE VESSEL

FIGURE I TYPICAL ELLIPTICAL FLAWS IN STRUCTURAL COMPONENTS

penetration of a shallow* semi-elliptical crack in a tension plate. Among the several solutions on the "surface flaw problem" as well as embedded flaws which have been published to date, the mathematically more rigorous solutions are all based on the alternating technique suggested by Kantorovich and Krylov[2]. This procedure was first applied to crack problems by Smith[3] who determined the stress intensity factors of a semi-circular crack in a thick beam in tension, bending, and subjected to rapid heating or cooling. This method of approach was then used by Smith and his coworkers to analyze a family of problems involving circular flaws and part-circular flaws[4,5,6]. Recently Hartranft and Sih[7] reexamined one of Smith's original solutions[3,8] with an added singularity function which increased the accuracy of their solution.

The disadvantage of using the circular crack solution is its geometry which cannot be used to model oblong elliptical or semi-cracks such as those shown in Figs. 1a and 1d[9]**. For better modeling of elliptical flaws, Shah and Kobayashi[9] used the potential function of Segedin[10] to derive a polynomial representation of the internal pressure on an elliptical crack. This solution was then used in the alternating method to determine the stress intensity factors of embedded elliptical flaws under nonuniform loadings[11]

---

*   Shallow crack means that the crack depth is less than half of the plate thickness.

** Part elliptical cracks, such as those shown in Figs. 1b and 1c, can be approximated by part circular crack as shown in Ref. 8. Part elliptical crack with large aspect ratio, i.e., $b/a \leq 0.2$, cannot be conveniently approximated by a part circular crack.

as well as to estimate the stress intensity factors for semi-elliptical surface flaws[14]. Prior to the above development, Kassir and Sih[15] determined the stress intensity factor of an elliptical crack under linearly varying internal pressure and uniform shear tractions. Smith[16] extended Kassir and Sih solution[15] following the procedure described in Ref. 9 to derive a polynomial distribution of shear tractions prescribed on an elliptical crack. In addition, Smith[17] has recently used this procedure to determine the stress intensity factor of a surface flaw in a thin tension plate.

The solution procedure involving an elliptical crack is convenient for modeling actual flaw geometries. The small number of derivable terms in the polynomial representation of the internal pressure, however, limits the accuracy in which a complex residual pressure distribution on the crack surface can be fitted. Unfortunately numerical convergence of the alternating method is sensitive to this fitting and thus the accuracy of the entire solution procedures hinges on the accuracy of fitting. In particularly, numerical difficulties in fitting residual stress are encountered in surface flaw problems where a portion of the ellipse protrudes through the free surface.

The purpose of this paper is to discuss numerical problems associated with the fitting process and to suggest procedures which reduce some of the immense amount of theoretical derivations and computer programming associated with this numerical analysis.

THEORETICAL BACKGROUND

Two solutions are needed in applying the alternating method to fracture mechanics problems involving elliptical cracks. One solution involves a semi-infinite solid and the other solution involves an elliptical crack both subjected to variable surface tractions. For elliptical crack problems involving flat surfaces, Love's solution[18,19] is used for the free-surface solution of the former. Numerical procedures related to Love's solution are well documented[3,4,8,11,14] and will not be repeated here. A discussion, however, on the tolerable maximum size of a rectangle for erasing the residual surface traction on the flat surface will be presented later.

In the following, a brief review of the basic equations for an elliptical crack with prescribed internal pressure[9], which can be represented by a polynomial in terms of Segedin's potential function[10], is presented.

Consider an elastic solid containing an elliptical crack, as shown in Fig. 2, which is located in the plane $z=0$, and is opened by applying an internal pressure, $p(x,y)$, symmetrically to both surfaces of the crack. The boundary conditions for this problem are:
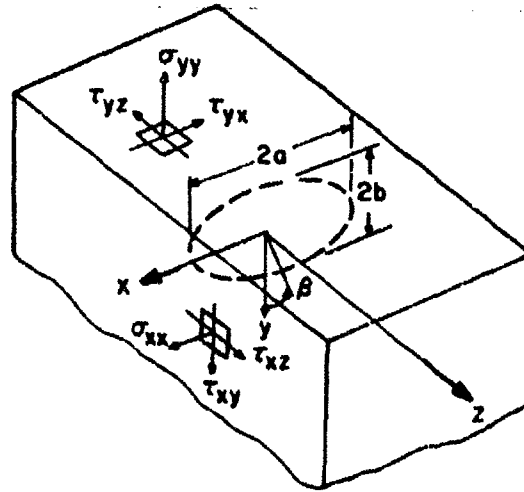
4

FIGURE 2. ELLIPTICAL CRACK IN A FINITE SOLID

$$\sigma_{zz} = -p(x,y) \qquad (\frac{x^2}{a^2} + \frac{y^2}{b^2} < 1, \; z = 0) \qquad (1a)$$

$$w = 0 \qquad (\frac{x^2}{a^2} + \frac{y^2}{b^2} > 1, \; z = 0) \qquad (1b)$$

$$\tau_{xz} = \tau_{yz} = 0 \qquad (z = 0) \qquad (1c)$$

$$\sigma_{xx} = \sigma_{yy} = \sigma_{zz} = \tau_{xy} = \tau_{yz} = \tau_{zx} = 0 \text{ at infinity} \qquad (1d)$$

For the vanishing shear stresses on $z=0$ plane and in the absence of body forces, Navier's equations of equilibrium are satisfied by the harmonic function of ϕ. The displacement perpendicular to the crack plane in terms of ϕ is,

$$w = z \frac{\partial^2 \phi}{\partial z^2} - 2(1-\eta) \frac{\partial \phi}{\partial z} \qquad (2)$$

where η is the Poisson's ratio. The stress components necessary for solving the surface flaw problem are given by,

$$\sigma_{yy} = 2G \left[z \frac{\partial^3 \phi}{\partial y^2 \partial z} + \frac{\partial^2 \phi}{\partial y^2} + 2\eta \frac{\partial^2 \phi}{\partial x^2} \right] \qquad (3a)$$

$$\sigma_{zz} = 2G \ [z \ \frac{\partial^3\phi}{\partial z^3} - \frac{\partial^2\phi}{\partial z^2}] \tag{3b}$$

$$\tau_{xy} = 2G \ [z \ \frac{\partial^3\phi}{\partial x\partial y\partial z} + (1-2\eta) \ \frac{\partial^2\phi}{\partial x\partial y}] \tag{3c}$$

$$\tau_{xz} = 2G \ z \ \frac{\partial^3\phi}{\partial x\partial z^2} \tag{3d}$$

$$\tau_{yz} = 2G \ z \ \frac{\partial^3\phi}{\partial y\partial z^2} \tag{3e}$$

where G is the shear modulus.

Due to practical limitations in deriving additional terms in the polynomial representation of the pressure distribution, $p(x,y)$, only terms up through the third powers in x and y were derived as,

$$p(x,y) = \sum_{i,j=0}^{3} A_{ij} \ x^i \ y^j \ . \tag{4}$$

The harmonic function which satisfies the necessary boundary conditions was derived from Segedin's potential function. Details of the harmonic function and its derivatives are described in Refs. 9 and 14.

Finally, the stress intensity factor associated with ϕ can be obtained through a procedure described by Irwin[20] or Kassir and Sih[15]. Again details of this procedure are described in Refs. 9 and 14.

Finite Difference Calculation of Stresses

As mentioned earlier, the derivable terms in the Eq. 4 were limited to a third order polynomial in x and y due to practical considerations. Some of this difficulty can be removed if the partial derivatives in Eq. 3 can be replaced by numerical differentiations. Analytical expressions of $\partial^2\phi/\partial x^2$ etc., which are given in the Appendix of Ref. 9, were used to obtain the third partial derivatives of ϕ with respect to x, y and z. Analytical expressions of $\partial^2\phi/\partial x^2$ etc. were evaluated numerically at two locations of x and x + 0.001a etc. to compute $\partial^3\phi/\partial x^3$ etc. These numerical derivatives were then combined as per Eq. 3 to determine the stresses of σ_{yy}, τ_{yz} and τ_{yx} at various values of x and z on various y = constant planes. These numerical results were found to agree within three significant figures with corresponding stresses obtained previously[3,9].

The above numerical differentiation procedure has been extended to compute the same third partial derivatives from analytical expressions of $\partial\phi/\partial x$ etc. Preliminary results show that the same

6

excellent agreement between stresses, which were computed numeri-
cally and by the closed form procedure, exists except for regions
of high stress gradients where the elliptical crack front inter-
sects with the y = const. plane, e.g. y=0 plane, in Fig. 2. Effort
is currently underway to determine whether the average surface
traction acting on the small region surrounding such stress singu-
larity can exhibit numerically the same effect as the residual
singular surface traction as far as the free surface solution is
concerned. If such replacement is possible, then the average
stresses determined by the second numerical differentiations of
$\partial\phi/\partial x$, etc. can also be used to compute the residual surface trac-
tions on the bounding free surfaces.

Maximum Permissible Rectangle Size

The second step of the alternating technique is to eliminate
the residual surface traction on the bounding free surfaces. A
common procedure is to use Love's solution[18,19] for a half space
with prescribed uniform surface tractions on a rectangle in the
bounding plane. When the alternating technique was first used to
analyze surface flaw problems several years ago, the total number
of such rectangles was of the order of 540^3. Through numerical
experimentation, Smith has gradually reduced the numbers of these
rectangles to 180^6 and then to 71^{17}. Hartranft and Sih, on the
other hand, increased the number of rectangles to 1744 which to-
gether with the increased number of Fourier series used, resulted
in computing time of 8 hours to solve one problem. The purpose of
this section is to determine the maximum permissible rectangle size
which will yield reasonably accurate results of this second step of
of the alternating procedure.

Since the continuously varying residual surface tractions on
the bounding plane are to be replaced by uniform surface tractions
over each of the rectangles forming the bounding plane, the prob-
lem reduces to the difference in the resultant stresses due to
prescribed uniform or variable surface tractions on the rectangle.
This difference in resultant stresses can be estimated by examining
the stresses in a half space due to (1) a linearly varying stress
distribution over the rectangle on the bounding plane, and (2) a
uniform stress distribution over the rectangle. The uniform stress
distribution is in equilibrium with the linearly varying stress
distribution as shown in Fig. 3. The stress distributions at any
point in a semi-infinite plate due to a linearly varying or a uni-
form surface traction, σ_{yy} , over a segment 2d as shown in the
legend of Fig. 3 are given by the following equations[21].

$$\sigma_{zz} = -\frac{f_o}{\pi} \left\{\frac{y}{d} \ln \frac{y^2+(z-d)^2}{y^2+(z+d)^2} + \frac{2y(z-d)}{y^2+(z-d)^2} + \frac{z+d}{d} \tan^{-1} \frac{2dy}{y^2+z^2-d^2}\right\}$$
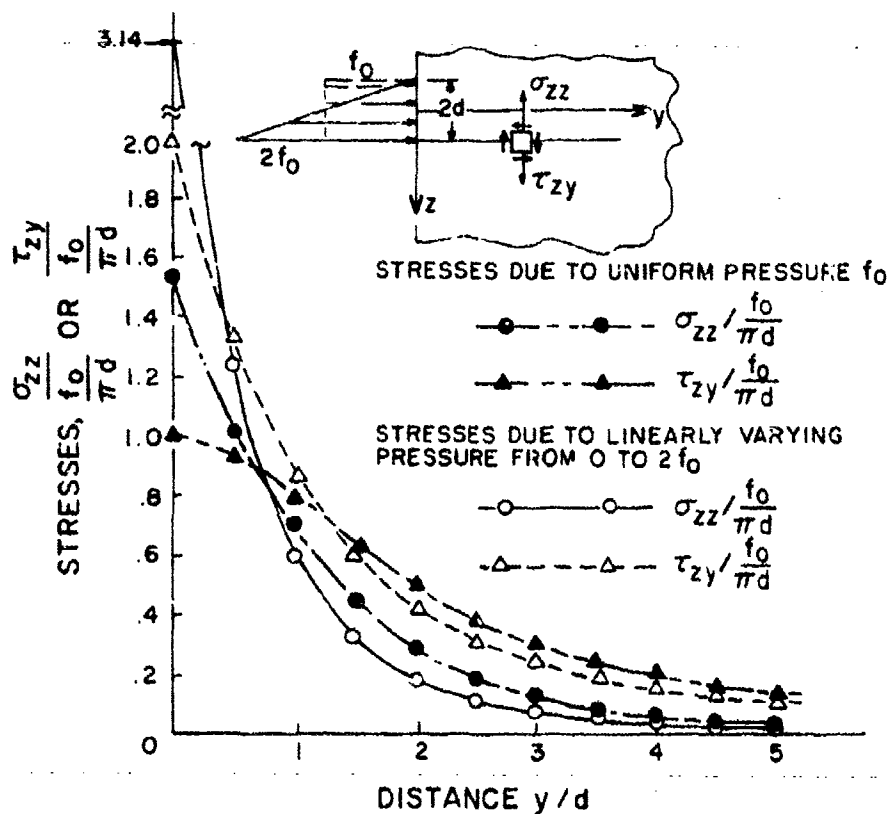
(5a)

FIGURE 3. STRESS DISTRIBUTION AT z = d IN A HALF PLANE DUE TO UNIFORM AND LINEARLY VARYING PRESSURES ACTING ON THE BOUNDING LINE.

$$\tau_{zy} = -\frac{f_o}{\pi} \left\{ \frac{2y^2}{y^2+(z-d)^2} - \frac{y}{d} \tan^{-1} \frac{2dy}{y^2+z^2-d^2} \right\} . \tag{5b}$$

For a uniform surface traction prescribed over a segment of 2d, these stresses become[21]

$$\sigma_{zz} = -\frac{f_o}{\pi} \left\{ \tan^{-1} \frac{2dy}{y^2+z^2-d^2} + \frac{2dy(\cdot y^2+z^2-d^2)}{[y^2+(z+d)^2][y^2+(z-d)^2]} \right\} \tag{6a}$$

$$\tau_{zy} = -\frac{f_o}{\pi} \frac{4dyz}{[y^2+(z+d)^2][y^2+(z-d)^2]} . \tag{6b}$$

Figure 3 shows the distributions of σ_{zz} and τ_{zy} at distances of z = d from the center of the load segment for linearly varying and uniform normal tractions acting on the segment. Although the stresses due to the two loads differ by a factor of 2 at y = 0 in

Fig. 3, this difference when superimposed on to other stresses due to the common uniform load acting on the rectangle, reduces the overall differences to less than 5% in actual computations. Further evaluations of Eqs. 5 and 6, for most parts of the elliptical crack, show that the differences in both normal and shear stresses on the crack plane due to the above two surface tractions rapidly diminish at a distance which is half-width away from the load segment.

The above results indicate that the size of the rectangle can be equal to its closest distance to the crack plane or to the other bounding surfaces for the case of a finite thickness solid, whichever is smaller. Similar criterion was found to hold for tangential surface traction acting on the bounding free surface. The number of necessary rectangles can be reduced systematically following this criterion thus resulting in substantial reduction in computing time.

Residual Pressure Distribution on Semi-Elliptical Crack

Another recognized drawback of the alternating technique based on the elliptical crack potential function is in its inability to approximate the residual pressure distribution on the crack surface with the limited third order polynomial. This drawback is for all practical purposes nonexistent for totally embedded elliptical flaw, such as those shown in Figs. 1a and 1d, since the residual pressure distribution varies smoothly. A third degree polynomial can be fitted within 5 percent of such residual pressure distribution and thus the numerical procedure converges rapidly with typical incremental change in the stress intensity factor to be less than 0.2 percent of the original stress intensity factor after 2 to 5 iterations.

For a surface flaw where the elliptical circle penetrates the free surface, this fitting problem becomes acute since the residual pressure on the crack surface normally reaches a maximum value in the vicinity of the free bounding surface. The physical crack obviously does not continue beyond the bounding surface while the elliptical crack, used in the alternating method, does protrude into this free space. In order to represent the free bounding surface, Hartranft and Sih[7] have suggested the use of only even terms of polynomial which reduces Eq. 4 to $\sigma_{zz} = A_{00} + A_{20} x^2 + A_{02} y^2$ to which the residual pressure distribution must be fitted. The result is an incomplete erasure of the residual pressure distribution resulting in slow convergence or possible divergence of the iteration process in the alternating procedure.

In a recent paper, one of the authors[2] showed that the stress intensity factor for a circular crack of radius b embedded in an

infinite solid and subjected to linearly varying pressure distribution of $\sigma_{zz} = p_0 (1 - \frac{y}{b})$ was approximately 5 percent higher than that of a semi-circular surface crack subjected to the same pressure distribution between $0 \leq y \leq b$. This empirical finding indicated that the stress intensity magnification factor due to the free bounding surface had an effect similar to continuing the linearly varying pressure distribution in the $-b \leq y \leq 0$ region of the fictitious portion of the semi-circular crack. This approximation would obviously result in a significant error in estimation of the stress intensity magnification factor if a similar procedure were used to continue into the region of $-b \leq y \leq 0$, the nonlinear pressure distribution acting on a semi-circular crack.

The above empirical finding led to further numerical experimentation for arriving at an optimum pressure distribution on the crack surface extended into the region of $-b \leq y \leq 0$ of the elliptical crack. Three pressure distributions of linear, quadratic, and cubic with the maximum pressure at the free surface, as shown in Fig. 4 were considered. For two-dimensional problems the stress intensity factors associated with an edge crack with linear, quadratic, and cubic pressure distributions, shown in Figs. 4a, 4c, and 4e, can be computed by using the results of Stallybrass[23]. In order to obtain the same stress intensity factor at the crack tip of a totally embedded through crack, various linear distributions of pressures were prescribed on the other half of the embedded crack, i.e., $-b \leq y \leq 0$. It was found that pressure distributions shown in Figs. 4b, 4d, and 4f yielded stress intensity factors which were reasonably close to those for the edge crack[*]. These pressure distributions were then prescribed onto the other half of the elliptical crack, i.e., $-b \leq y \leq 0$, where half of the crack was loaded by linear, quadratic, or cubic pressure distributions. Six terms in Eq. 4 or $\sigma_{zz} = A_{00} + A_{01}y + A_{20}x^2 + A_{02}y^2 + A_{21}x^2y + A_{03}y^3$ were then least square fitted to this prescribed pressure distribution on the crack surface.

The above procedure of least square fitting was also applied to the two-dimensional problem illustrated in Fig. 4. For this purpose, a pressure of $\sigma_{zz} = A_0 + A_1y + A_2y^2 + A_3y^3$ was fitted to the 3 pressure distributions illustrated in Figs. 4b, 4d, and 4f. Table I shows the fitted stress distributions, stress intensity factors at the right crack tip, and the corresponding stress intensity factors for edge cracks.

---

[*] Stress intensity factors at the right crack tip were computed by the procedure described in Ref. 24.

$K = 0.4385 p_o \sqrt{\pi b}$

(a)

$K = 0.4385 p \sqrt{\pi b}$

(b)

$K = 0.5959 p_o \sqrt{\pi b}$

(c)

$p(y) = p_o \left(1 - \frac{y^2}{b^2}\right)$

$K = 0.5446 p_o \sqrt{\pi b}$

(d)

$K = 0.6071 p_o \sqrt{\pi b}$

(e)

$p(y) = p_o \left(1 - \frac{y^3}{b^3}\right)$
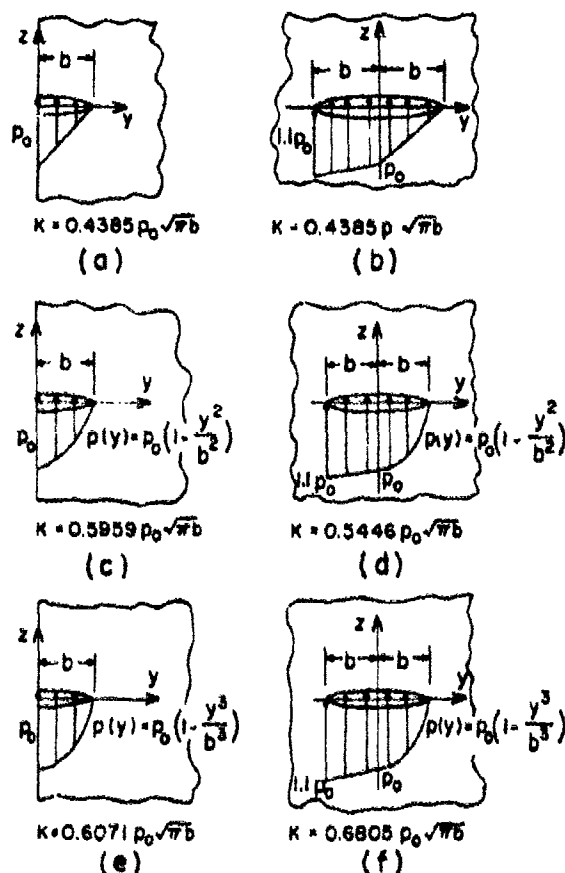
$K = 0.6805 p_o \sqrt{\pi b}$

(f)

FIGURE 4. STRESS INTENSITY FACTOR FOR AN EDGE CRACK SUBJECTED TO VARIABLE PRESSURE LOADING

Differences between the respective stress intensity factors can obviously be reduced by further numerical experimentation with various pressure distributions prescribed in the region of $-b \leq y \leq 0$. The purpose of this study, however, was to demonstrate that reasonable results can be obtained for the three cases of prescribed linear, quadratic, and cubic pressure distributions with the same additional pressure in the region of $-b \leq y \leq 0$ and thus no further attempt was made to improve the accuracy of the resultant stress intensity factors.

TABLE I

Prescribed Pressure	Fitted Pressure	K_I(Right crack tip)	K_I(Edge Crack)
Linearly Varying Fig. 4b	$\sigma_{zz} = 0.9960 - 0.8714y - 0.4480y^2 + 0.3350y^3$	$0.4636\ p_o \sqrt{\pi b}$	$0.4385\ p_o \sqrt{\pi b}$
Quadratically Varying Fig. 4d	$\sigma_{zz} = 1.0042 - 0.1843y - 0.4937y^2 - 0.4094y^3$	$0.5169\ p_o \sqrt{\pi b}$	$0.5959\ p_o \sqrt{\pi b}$
Cubically Varying Fig. 4f	$\sigma_{zz} = 0.9965 + 0.1508y - 0.4480y^2 - 0.7276y^3$	$0.5808\ p_o \sqrt{\pi b}$	$0.6071\ p_o \sqrt{\pi b}$

Figure 5 shows the normalized stress intensity factor of a circular crack for the pressure distribution shown in Fig. 4b. Poisson's ratio for this analysis was set to $\eta = 0.3$. The polynomial pressure distribution fitted within 2% of the prescribed bilinear pressure distribution. As shown in Fig. 5, the stress intensity factor thus obtained differed as much as 9% from the corresponding stress intensity factor for a semi-circular surface crack with a prescribed linearly varying load. Part of this difference, i.e., approximately 2%, can be attributed to the differences in the Poisson's ratios used in the two analyses[8].

It is interesting to note that the residual normal surface tractions, σ_{yy}, on the y = 0 plane for the problem illustrated in the legend of Fig. 4 are nearly equal to the corresponding residual normal tractions for a circular crack subjected to uniform pressure of p_0. It appears then that the additional residual tangential surface tractions, $\tau_{yz}]_{y=0}$, in this problem act to counteract the crack opening moments of the residual normal surface tractions thus causing the resultant stress intensity factor to approach that of a semi-circular crack in a semi-infinite solid and subjected to linearly varying pressure.

The close agreement between the stress intensity factors for the two extremes of a semi-circular crack and a two-dimensional edge crack suggested that this procedure of prescribing appropriate
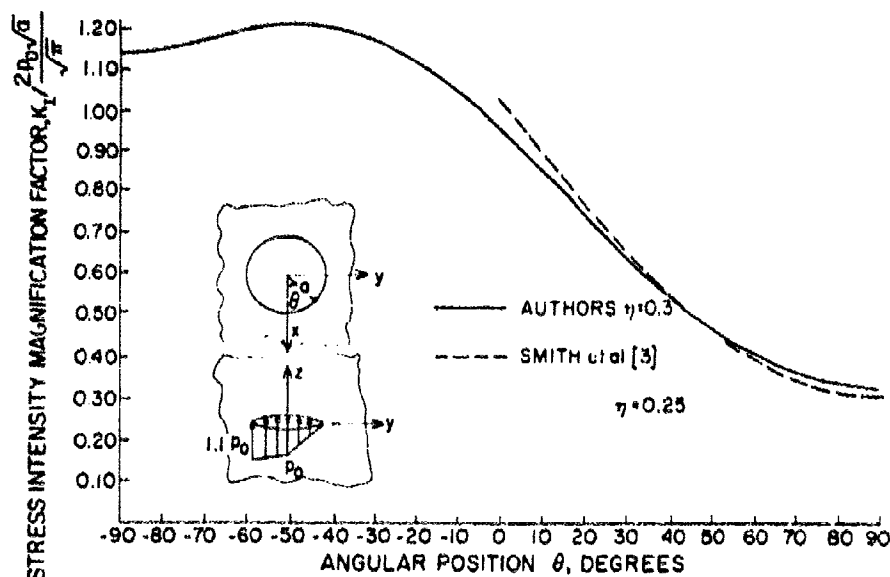

FIGURE 5. STRESS INTENSITY FACTORS FOR A CIRCULAR CRACK SUBJECTED TO A COMBINED TWO LINEAR VARYING PRESSURE DISTRIBUTIONS AND A SEMI-CIRCULAR SURFACE CRACK WITH LINEARLY VARING LOAD

12

pressure distribution in the region of $-b \leq y \leq 0$ of an elliptical crack can be used to estimate the stress intensity factors for semi-elliptical surface flaws subjected to linearly varying pressure distribution. The estimated stress intensity magnification factors thus obtained along the periphery of a semi-elliptical crack subjected to linearly varying pressure distribution are shown in Fig. 6. The stress intensity factor in the vicinity of $\theta = 0$, i.e., where the semi-elliptical crack meets the free bounding surface, is not shown since the stress singularity at this point is believed to vanish following the analysis by Hartranft and Sih[7]. The error bounds of this estimation are indicated in Fig. 6 by the two known stress intensity factors for $b/a = 0$ and
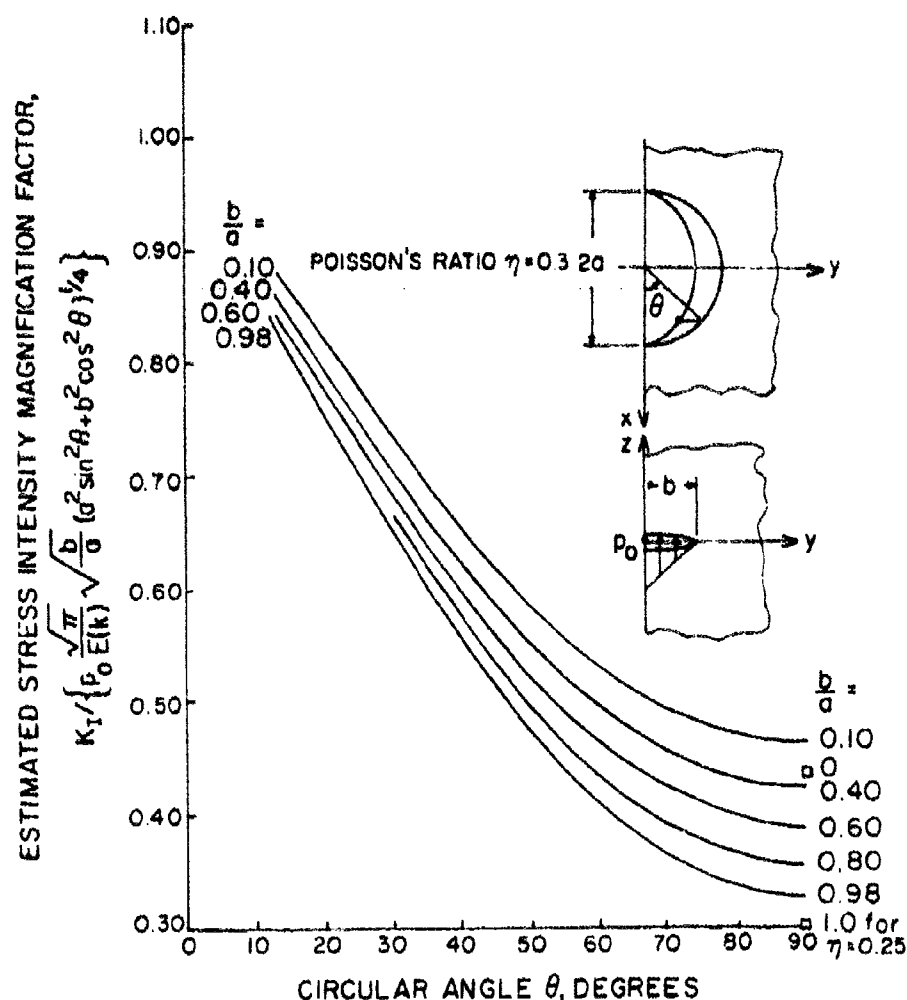

FIGURE 6. ESTIMATED STRESS INTENSITY FACTOR OF A SEMI-ELLIPTICAL FLAW IN A HALF SPACE SUBJECTED TO LINEARLY VARYING LOAD.

1.0. The overestimation in the stress intensity magnification factors at the deepest penetration of the ellipse or $\theta = 90°$ is consistent with the corresponding two-dimensional problem shown in Table I. For a better estimate of the stress intensity magnification factor at this position, all values could be lowered 7% following the results in Table I.

The same procedure was used to estimate the stress intensity magnification factors for semi-elliptical cracks subjected to quadratic and cubic distributions of pressure. Again, the fitted polynomial distribution of pressure fitted within 2 percent of the prescribed pressure. Unlike the previous case of linearly varying pressure distribution, the stress intensity factors for quadratic and cubic pressure distribution on a semi-circular surface flaw are not known. The obtained stress intensity factors, however, were consistent with known theoretical solutions at one extreme of $b/a = 0$, i.e., for an edge crack.

DISCUSSION

The stress intensity factor of a semi-elliptical crack in a semi-infinite solid subjected to uniaxial tension can be estimated from the results of Fig. 5. Figure 7 shows the pressure distribution for erasing the residual, normal stresses on the free surface at $y=0$ of a semi-infinite solid after the first iteration in the alternating method. An equivalent linearly varying pressure distribution as shown in Fig. 7, which is nearly in equilibrium with the rapidly varying pressure distribution is now considered. The stress intensity factor for a semi-elliptical crack subjected to the equivalent linearly varying pressure distribution is then estimated from Fig. 6. The superposition of this stress intensity factor to the original stress intensity factor of an elliptical crack in an infinite solid and subjected to uniform pressure then yields an estimate of the front surface magnification factor for a semi-elliptical crack in a semi-infinite solid as shown in Fig. 8. It should also be noted that, as evident from the equivalent pressure distributions in Fig. 7, this procedure will yield underestimated stress intensity magnification factors close to the free surface. Nevertheless, for a semi-circular crack, the estimated value of $M_F = 1.13$ at an angular orientation of $\theta = 20°$ is sufficiently close to the original results of $M_F = 1.12$ obtained by Smith et al.[3]

The estimated front surface stress intensity magnification factors together with those by Smith and Alavi[5], Kobayashi and Moss[25], and Nisitani and Murakami[20] are shown in Fig. 9. The latter results by Nisitani and Murakami, which were computed for Poisson's ratio of $\eta = 0$, were corrected for $\eta = 0.25$, as shown in Fig. 9 following an investigation on the effects of Poisson's
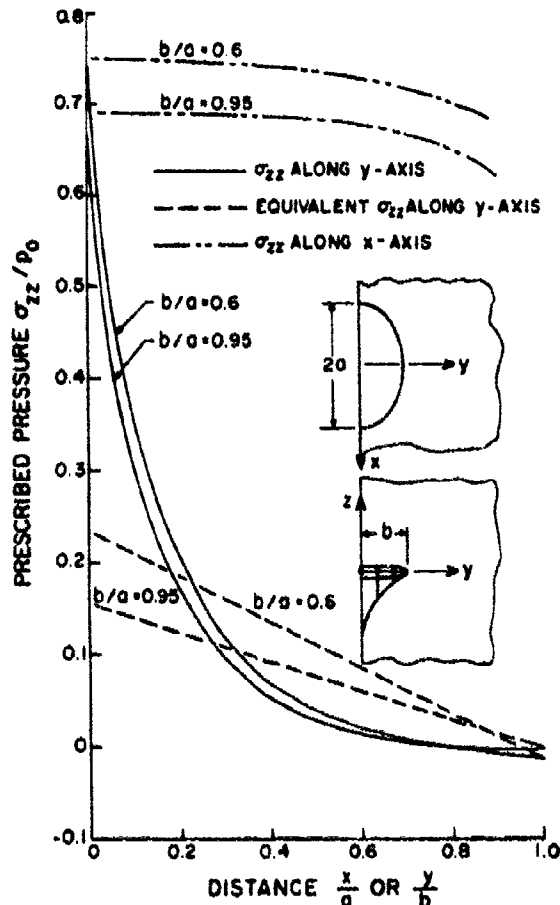
14

FIGURE 7. PRESCRIBED PRESSURE DISTRIBUTION ON A SEMI-
ELLIPTICAL CRACK SURFACE AFTER FIRST ITERATION
IN THE ALTERNATING METHOD, POISSON RATIO η=0.3

ratio by Shah and Kobayashi[?]. Also shown in Fig. 9 is the single result by Hartranft and Sih for $\eta = 0.30$[7]. Although the new estimates of the front surface magnification factor appear to be in closer agreement with the results by Smith and Alavi[5], when an adjustment is made to account for the possible overestimation discussed previously, the adjusted front surface stress intensity magnification factor will move closer to the analytically more rigorous results by Nisitani and Murakami.

The above mentioned approximate procedure does not eliminate the difficulties in fitting a polynomial pressure distribution. Much of these difficulties, however, can be reduced by a shrewd use of the limited terms in the polynomial using numerical procedures akin to over-and-under relaxations.

The alternating procedure with optimum rectangle spacing on the free bounding surface and the pressure distribution in the region of $-b \leq y \leq 0$ of the elliptical crack are being used to solve practical problems involving semi-elliptical surface flaws. Hopefully, these results will be available for presentation at the Conference of Prospects of Fracture Mechanics.
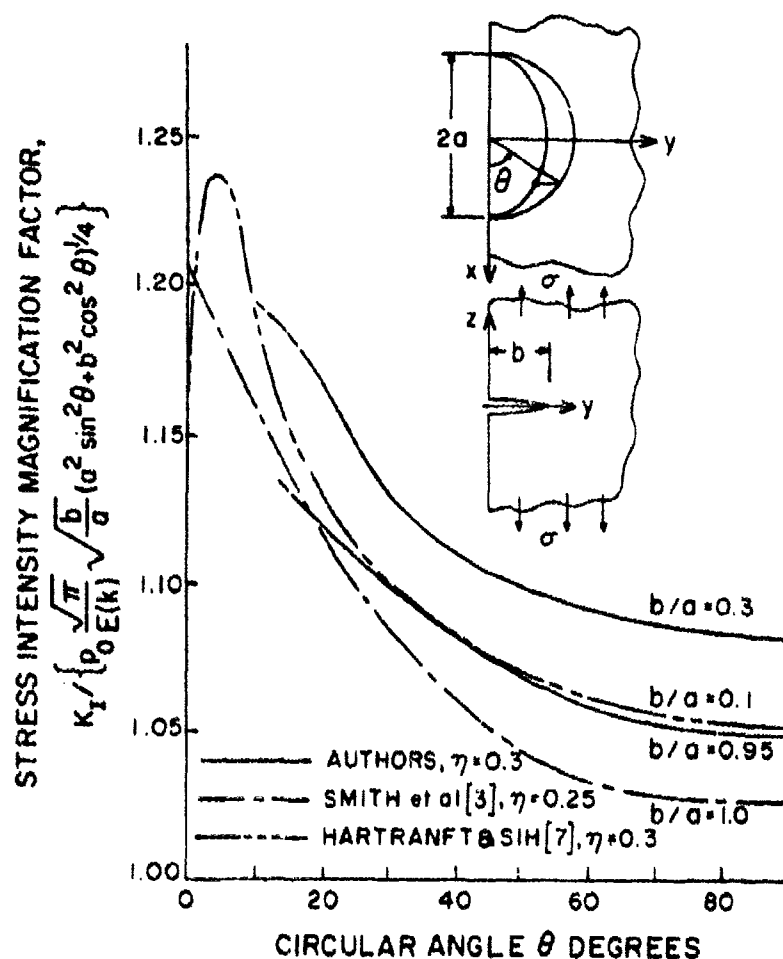
ACKNOWLEDGEMENT

FIGURE 8. STRESS INTENSITY MAGNIFICATION FACTOR ALONG THE PERIPHERY OF SEMI-ELLIPTICAL SURFACE CRACK IN A SEMI-INFINITE SOLID SUBJECTED TO UNIAXIAL TENSION.

REFERENCES

1. Irwin, G.R., The Crack Extension for a Part-Through Crack in a Plate, J. of Appl. Mech., Trans. of ASME, 29, 651, 1962.
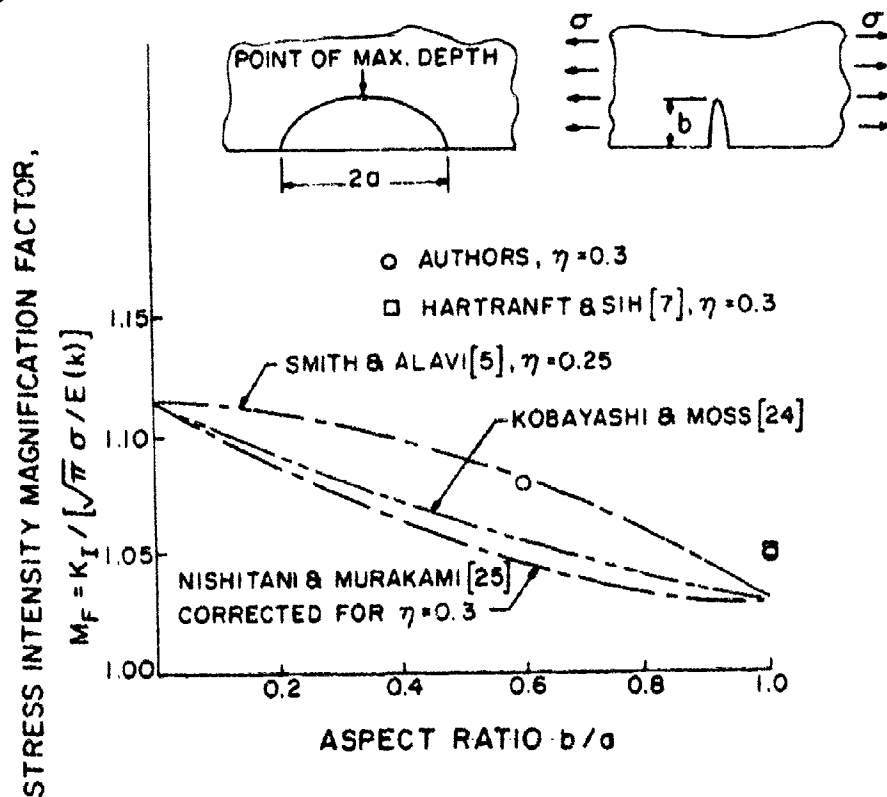
FIGURE 9. STRESS INTENSITY MAGNIFICATION FACTOR AT POINT OF MAXIMUM DEPTH OF A SEMI-ELLIPTICAL CRACK IN A SEMI-INFINITE SOLID SUBJECTED TO UNIAXIAL TENSION.

2. Kantorovich, L.V. and Krylov, V.L., _Approximate Methods of Higher Analysis_, Interscience, New York, 1964.

3. Smith, F.W., Emery, A.F. and Kobayashi, A.S., Stress Intensity Factors for Semi-Circular Cracks, _J. of Appl. Mech., Trans. of ASME_, _34_, 953, 1967.

4. Smith, F.W., and Alavi, M.J., Stress Intensity Factors for a Penny-Shaped Crack in a Half Space, _J. of Engrg. Fracture Mechanics_, _3_, 241, 1971.

5. Smith, F.W., and Alavi, M.J., Stress Intensity Factors for a Part-Circular Surface Flaw, Proc. of 1st Int'l. Conf. on Pressure Vessel Technology, Delft, Holland, 1969.

6. Thresher, R.W., and Smith, F.W., Stress Intensity Factors for a Surface Crack in a Finite Solid, J. of Appl. Mech., Trans. of ASME, 29, 195, 1972.

7. Hartranft, R.J., and Sih, G.C., Alternating Method Applied to Edge and Surface Crack Problems, Methods of Analysis and Solutions of Crack Problems (G.C. Sih, editor), Noordhoff Int'l., Leyden, Holland, 179, 1973.

8. Smith, F.W., The Elastic Analysis of the Part-Circular Surface Flaw Problem by the Alternating Method, The Surface Crack: Physical Problems and Computational Solutions (J.L. Swedlow, editor), ASME, New York, 125, 1972.

9. Segedin, C.M., A Note on Geometric Discontinuities in Elastostatics, Int'l. J. of Engrg. Science, 6, 309, 1968.

10. Shah, R.C., and Kobayashi, A.S., Stress Intensity Factor for an Elliptical Crack under Arbitrary Normal Loading, J. of Engrg. Fracture Mechanics, 3, 71, 1971.

11. Shah, R.C., and Kobayashi, A.S., Stress Intensity Factors for an Elliptical Crack Approaching the Surface of a Semi-Infinite Solid, Int'l. J. of Fracture, 9, 133, 1973.

12. Shah, R.C., and Kobayashi, A.S., Stress Intensity Factors for an Elliptical Crack Approaching the Surface of a Plate in Bending, Stress Analysis and Growth of Cracks, ASTM STP 513, 1, 1972.

13. Shah, R.C., and Kobayashi, A.S., Elliptical Crack in a Finite Thickness Plate Subjected to Tensile and Bending Loading, to be published in the J. of Engrg. for Industry, Trans. of ASME, 1974.

14. Shah, R.C., and Kobayashi, A.S., On the Surface Flaw Problem, The Surface Crack: Physical Problems and Computational Solutions (J.L. Swedlow, editor), ASME, 125, 1972.

15. Kassir, M.K., and Sih, G.C., Three-Dimensional Stress Distribution Around an Elliptical Crack under Arbitrary Loadings, J. of Appl. Mech., Trans. of ASME, 33, 601, 1966.

16. Smith, F.W., and Sorensen, D.R., The Elliptical Crack Subjected to Nonuniform Shear Loading, to be published in the J. of Appl. Mech., Trans. of ASME.

18

17. Smith, F.W., and Sorensen, D.R., The Semi-Elliptical Surface Crack--A Solution by the Alternating Method, Colorado State Univ. Tech. Rept. 4, August 1973, NASA Grant NGL-06-002-063.

18. Love, A.E.H., On Stress Produced in a Semi-Infinite Solid by Pressure on Part of the Boundary, Phil. Trans. of the Roy. Soc., Series A, 228, 387, 1929.

19. Love, A.E.H., A Treatise on the Mathematical Theory of Elasticity, Dover Publications, New York, 241, 1944.

20. Irwin, G.R., Analytical Aspects of Crack Stress Field Problems, Univ. of Illinois T. and A.M. Rept. No. 213, 1962.

21. Durelli, A.J., Phillips, E.A., Tsao, C.H., Introduction to the Theoretical and Experimental Analysis of Stress and Strain, McGraw-Hill, 225, 1958.

22. Kobayashi, A.S., A Simple Procedure for Estimating the Stress Intensity Factors in Region of High Stress Gradient, Proc. of US-Japan Seminar 1973, Significance of Defects in Welded Structures (T. Kanazawa and A.S. Kobayashi, editors), Univ. of Tokyo Press, March 1974.

23. Stallybrass, M.P., A Crack Perpendicular to an Elastic Half-Plane, Int'l. J. of Engrg. Sciences, 8, 351, 1970.

24. Paris, P.C., and Sih, G.C., Stress Analysis of Cracks, Fracture Toughness and Its Applications, ASTM STP 381, 30, 1965.

25. Kobayashi, A.S., and Moss, W.L., Stress Intensity Magnification Factors for Surface-Flawed Tension Plate and Notched Round Tension Bar, Proc. of the 2nd Int'l. Conf. on Fracture, 31, 1969.

26. Nisitani, H., and Murakami, Y., Stress Intensity Factor of an Elliptical Crack or a Semi-Elliptical Crack Subjected to Tension, to be published in the Int'l. J. of Fracture.

27. Shah, R.C., and Kobayashi, A.S., Effect of Poisson's Ratio on Stress Intensity Magnification Factor, Int'l. J. of Fracture, 9, 360, Sept. 1973.